Chinese Chemical Letters 37 (2026) 111706

Contents lists available at ScienceDirect

Chinese Chemical Letters

journal homepage: www.elsevier.com/locate/cclet

Enhancing the phosphorescence performance of organic doped system by carbonylation of guests

Lei Wang[a], Jianing Zhang[a], Jin Xiong[a], Wenbo Dai[a,c], Miaochang Liu[a], Xiaobo Huang[a], Yuye Chai[a,*], Yunxiang Lei[a,c,*], Zhengxu Cai[d], Minyu Zhu[b,*]

[a] School of Chemistry and Materials Engineering, Wenzhou University, Wenzhou 325000, China
[b] Department of Orthopedics (Spine Surgery), First Affiliated Hospital of Wenzhou Medical University, Wenzhou 325000, China
[c] Key Lab of Biohealth Materials and Chemistry of Wenzhou, Wenzhou 325035, China
[d] Beijing Key Laboratory of Construction Tailorable Advanced Functional Materials and Green Applications, School of Materials Science and Engineering, Beijing Institute of Technology, Beijing 100081, China

ARTICLE INFO

Article history:
Received 12 May 2025
Revised 9 August 2025
Accepted 10 August 2025
Available online 11 August 2025

Keywords:
Room temperature phosphorescence
Host-guest doped system
Carbonyl induced emission
Hydrogen bonds
Bioimaging

ABSTRACT

The host-guest doped strategy has become the main method for constructing organic phosphorescence materials. In the doped system, guest molecules emit phosphorescence, therefore, improving the luminescence performance of guests is the key to optimizing the phosphorescence property of the doped materials. Herein, we designed to introduce the carbonyl group on the guest molecules. Carbonyl group can effectively promote n-π^* transitions, thereby increasing the spin-orbit coupling (SOC) constant of the guests, ultimately improving the phosphorescence performance of the doped materials. Using the indazole derivative (IZ) as the initial guest, two other guests containing carboxyl group (IZ-CG) or ethoxycarbonyl group (IZ-EG) were successfully obtained. Further selected two small molecules and two polymers as the hosts to construct four doped systems. Among these doped systems, the phosphorescence performance of doped materials with IZ-CG or IZ-EG as the guest is significantly better than that of doped materials with IZ as the guest. The phosphorescence lifetime has increased by 2.3-5.0 times, and the phosphorescence quantum yield has increased by 3.0-5.7 times. Theoretical calculations and single crystal structures indicated that carbonyl groups can not only increase the SOC constant, but also enhance the intermolecular interactions of the guests. In addition, doped material can be effectively used for imaging subcutaneous and lymph nodes in mice, achieving a high signal-to-noise ratio.

© 2026 Published by Elsevier B.V. on behalf of Chinese Chemical Society and Institute of Materia Medica, Chinese Academy of Medical Sciences.

Organic room temperature phosphorescence (RTP) materials have garnered significant attention in recent years within the fields of biological imaging [1–5], flexible electronic devices [6–11], information encryption and advanced anti-counterfeiting [12–14]. The radiative transition of triplet excitons in RTP materials enables long-persistent luminescence, effectively avoiding the common issue of background fluorescence interference seen in fluorescence materials, thereby significantly enhancing imaging and display clarity and sensitivity. In addition, the long-lifetime nature of RTP materials provides distinct advantages in time-resolved imaging and applications under low-light conditions. However, the practical application of RTP materials still faces several challenges, with the most critical being how to effectively enhance phosphorescence efficiency and stability. Enhancing phosphorescence efficiency relies on two key processes: First, accelerating intersystem crossing (ISC) from singlet to triplet states, and second, suppressing non-radiative decay of triplet excitons [15–17]. The ISC process is the critical step in converting excited singlet excitons into triplet excitons, while non-radiative decay of triplet excitons is the primary cause of reduced phosphorescence efficiency. Therefore, optimizing the two processes through molecular design and modulation is key to improving the performance of organic phosphorescence materials. To achieve strong phosphorescence emission, researchers have proposed various strategies, such as the heavy atom effect [18,19], hydrogen bonding [20–24], crystallization [25,26], host-guest complex doping [27–32], and ionic bonding [33–37]. Among these emerging techniques, the host-guest doped strategy has attracted widespread attention due to its low guest content which can reduce synthesis costs, diverse host options, and the strong intermolecular interactions between host-guest molecules. In most doped systems, the phosphorescence essentially originates from the guest molecules, while the host matrix facilitates

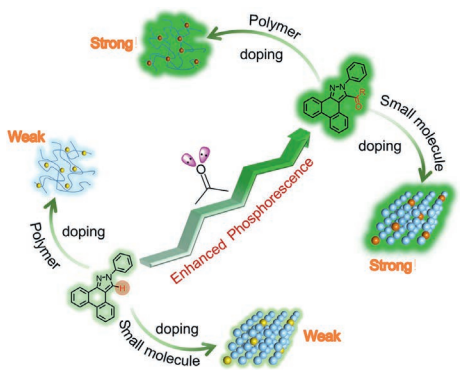
* Corresponding authors.
E-mail addresses: cyy@wzu.edu.cn (Y. Chai), yunxianglei@wzu.edu.cn (Y. Lei), zhuminyu@wzhospital.cn (M. Zhu).

https://doi.org/10.1016/j.cclet.2025.111706
1001-8417/© 2026 Published by Elsevier B.V. on behalf of Chinese Chemical Society and Institute of Materia Medica, Chinese Academy of Medical Sciences.

energy transfer and provides a rigid environment to suppress guest molecular motion, so the luminescence properties of the guests largely determine the optical characteristics of the doped system [38,39]. Therefore, enhancing the luminescent activity of the guests through molecular design engineering is an effective strategy to improve the phosphorescence performance of doped materials.

It is well established that the most critical photophysical processes in phosphorescence systems encompass intersystem crossing (ISC, rate constant K_{ISC}) and phosphorescence decay (rate constant K_P). Among the diverse strategies in molecular design, the n-π^* transitions have been extensively employed to improve K_{ISC} and K_P. The presence of n-π^* transitions can significantly reduce the fluorescence decay rate (rate constant K_F), thereby increasing the intersystem crossing quantum yield (Φ_{ISC}) of organic systems. Additionally, T_1 states with prominent n-π^* characteristics typically exhibit rapid phosphorescence decay (*i.e.*, a large K_P), effectively dissipating the energy of the triplet state. The most common strategy for promoting n-π^* transitions is the introduction of carbonyl groups, as their presence significantly influences the energy required for n-π^* transitions. Due to the high energy of the π^* orbital in carbonyl groups, the transition of n-electrons to the π^* orbital requires considerable energy. However, when carbonyl groups are connected to other moieties (*e.g.*, auxochromes), their interactions can markedly alter the n-π^* transition properties of carbonyl compounds. For instance, auxochromes can modulate the energy levels of the π^* orbital through conjugation, thereby altering the energy required for n-π^* transitions and promoting n-π^* transitions. This effectively increases the SOC constant of the guest molecules, thereby significantly enhancing the ISC capability of excitons. Furthermore, the introduction of carbonyl groups facilitates the formation of hydrogen-bonding networks, further enhancing the phosphorescence performance of doped systems. Therefore, incorporating carbonyl groups to enhance n-π^* transitions represent an effective strategy for improving the phosphorescence activity of doped materials (Scheme 1) [40–47].

Herein, we designed and synthesized the indazole derivative 2-phenyl-2*H*-benzo[*e*,*g*]indazole (IZ) as the initial guest molecular framework. Subsequently, carboxyl and ester groups were introduced into the framework, resulting two indazole derivatives (IZ-CG and IZ-EG) as other guests (Fig. 1a). The phosphorescence lifetime of IZ is 310 ms (77 K), while IZ-CG and IZ-EG have been extended to 1024 and 921 ms. In addition, the phosphorescence emission intensity (77 K) of IZ-CG and IZ-EG is also higher than that of IZ. Subsequently, small molecules phenyl benzoate (PB) and triphenylarsine (TPAs), along with polymers polyvinyl alcohol (PVA) and polylactic acid (PLA), were selected as hosts to construct four doped systems. Regardless of the host (PB, TPAs, PVA, or PLA) used for doping the guest IZ, the corresponding doped



Scheme 1. Schematic diagram of the host–guest doped system.

materials exhibited weak phosphorescence activity, with phosphorescence quantum yields (Q.Y.) of 2.78 %-7.20 % and the phosphorescence lifetimes of 10-620 ms. In contrast, the phosphorescence performance of doped materials incorporating carbonyl-modified IZ-CG and IZ-EG as guests was significantly improved. The phosphorescence quantum efficiency has been increased to 10.37 %-21.41 %, and the phosphorescence lifetime has been extended to 218-1690 ms. The theoretical calculation results demonstrated that the introduction of carbonyl groups significantly increasing the spin-orbit coupling (SOC) constant of guests, thereby enhancing the ISC capability of excitons. Moreover, it promoted the formation of hydrogen-bonding networks between the host and guest molecules, enhancing both the phosphorescence emission intensity and the lifetimes of the doped materials. Finally, the doped material IZ-CG/BP was successfully used for subcutaneous injection and lymph node imaging in mice, with a signal-to-noise ratio (SBR) of 50 and 31. This work successfully enhanced the phosphorescence activity of the doped system by carbonylating the guests, providing a new strategy for constructing doped materials with excellent phosphorescence properties.

The organic guest molecules IZ, IZ-CG and IZ-EG were synthesized following the reported method (Fig. 1a and Scheme S1 in Supporting information). The molecular structures and purities were verified using nuclear magnetic resonance spectroscopy, single-crystal X-ray diffraction, mass spectrum, and high-performance liquid chromatography (Fig. S1 in Supporting information). The guest IZ displayed blue fluorescence in solution state, with an emission wavelength of 365 nm (Fig. 1b). Due to the carbonyl group is an electron withdrawing group, the guests IZ-CG and IZ-EG transform into a D-A structure, resulting in the fluorescence wavelength redshift to about 420 nm (Fig. 1b). In addition, the phosphorescence wavelength also shifted from 463 nm to 490 nm (Fig. S2 in Supporting information). More importantly, the introduction of carbonyl groups significantly enhanced the phosphorescence emission intensity and lifetime of the guest molecules. From IZ to IZ-CG and IZ-EG, the phosphorescence intensity increased by 3.25 times and 3.50 times, respectively (Fig. 1c), the phosphorescence lifetime was extended from 0.31 s to 1.02 s and 0.92 s (Fig. 1d). Additionally, both the intensity and duration of the afterglow were substantially enhanced at 77 K (Fig. 1e). The above results fully demonstrated that the carbonyl groups had successfully improved the phosphorescence performance of guest molecules.

To investigate the influence of carbonyl compounds as guests on the phosphorescence performance of doped materials, we selected the small molecule phenyl benzoate (PB) and triphenylarsine (TPAs) as the hosts to construct the doped system, the doped materials were prepared using the melt-camethod. Given that the host-guest doping ratio significantly influences the phosphorescence performance of doped system [48–52], the doped materials IZ-EG/PB with varying guest-to-host molar ratios (1:50 to 1:10000) were prepared. The results shown that the phosphorescence emission intensity reached the maximum at a guest-to-host molar ratio of 1:500 was adopted for all doped materials (Fig. S3 in Supporting information). The absorption spectra and excitation spectra of the guest and doped material shown that the excitation wavelength for fluorescence emission was about 315 nm, and the excitation wavelength for phosphorescence emission was about 350 nm (Fig. S4 in Supporting information). The doped material IZ/PB exhibited blue fluorescence with an emission wavelength of 398 nm (Fig. S5 in Supporting information), with the fluorescence quantum yields (Q.Y.) of 12.3 % (Table S1 in Supporting information), upon removal of the excitation source, IZ/PB displayed a weak green afterglow about 1.5 s. Its phosphorescence wavelength was 490 nm (Fig. 2a), with a phosphorescence lifetime of 147 ms and a phosphorescence Q.Y. of 7.2 % (Figs. 2b and c). However, com-

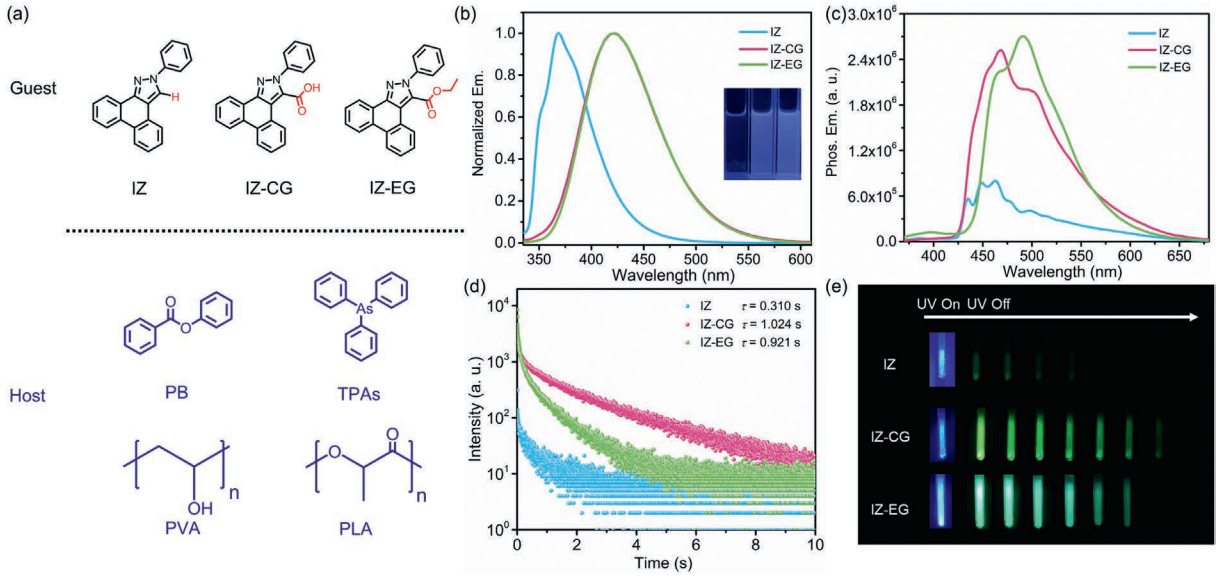


Fig. 1. (a) Molecular structures of the three guests and four hosts. (b) Fluorescence emission spectra of three guests in solution state (tetrahydrofuran as solvent; concentration: 1.0×10^{-5} mol/L; Ex. wavelength: 315 nm. Inset: Fluorescence images of three guests in solution state). (c) Phosphorescence emission spectra of three guests (77 K; Ex. wavelength: 350 nm, delayed time: 1 ms). (d) Emission intensity decay curves of three guests (77 K). (e) Afterglow images of three guests (77 K).

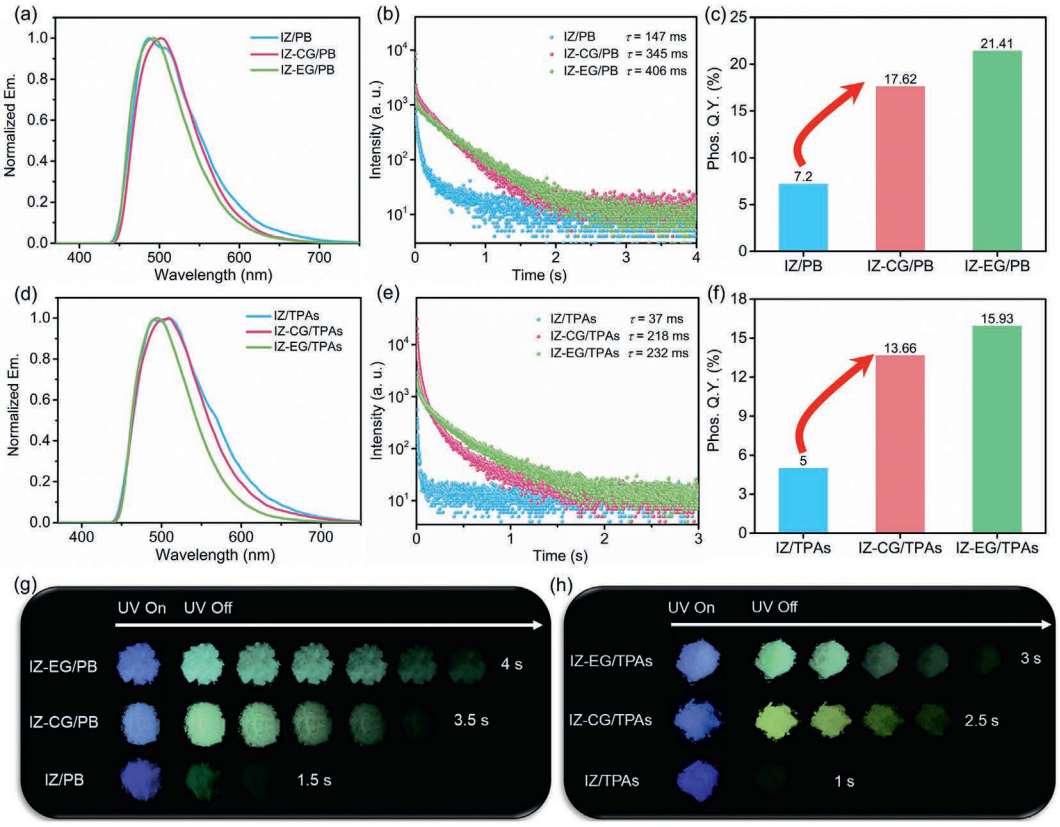


Fig. 2. Phosphorescence emission spectra (a), emission intensity decay curves (b) and phosphorescence Q.Y. (c) of PB-based doped materials. Phosphorescence emission spectra (d), emission intensity decay curves (e) and phosphorescence Q.Y. (f) of TPAs-based doped materials. (g) Luminescence pictures of PB-based doped materials before and after turning off the 365 nm light. (h) Luminescence pictures of TPAs-based doped materials before and after turning off the 365 nm light (Ex. of PB-based and TPAs-based doped materials: 350 nm, delayed time: 1 ms).

pared to the phosphorescence activity of IZ/PB, the two doped materials (IZ-CG/PB and IZ-EG/PB) incorporating carbonyl-modified molecules as guests exhibited superior phosphorescence performance. The phosphorescence lifetimes extended to 345 ms and 406 ms (Fig. 2b). Concurrently, the fluorescence Q.Y. increased to 33.29 % and 31.54 % (Table S1), and the phosphorescence quantum yields increased to 17.62 % and 21.41 % (Fig. 2c). Compared to IZ/PB, the phosphorescence lifetimes of IZ-CG/PB and IZ-EG/PB were extended by 2.35-fold and 2.76-fold, respectively, and the emission intensity increased by a factor of 2 and 3. For the doped system with TPAs as host, as anticipated, the phosphorescence performance was comparable to that of the PB-based doped materials.

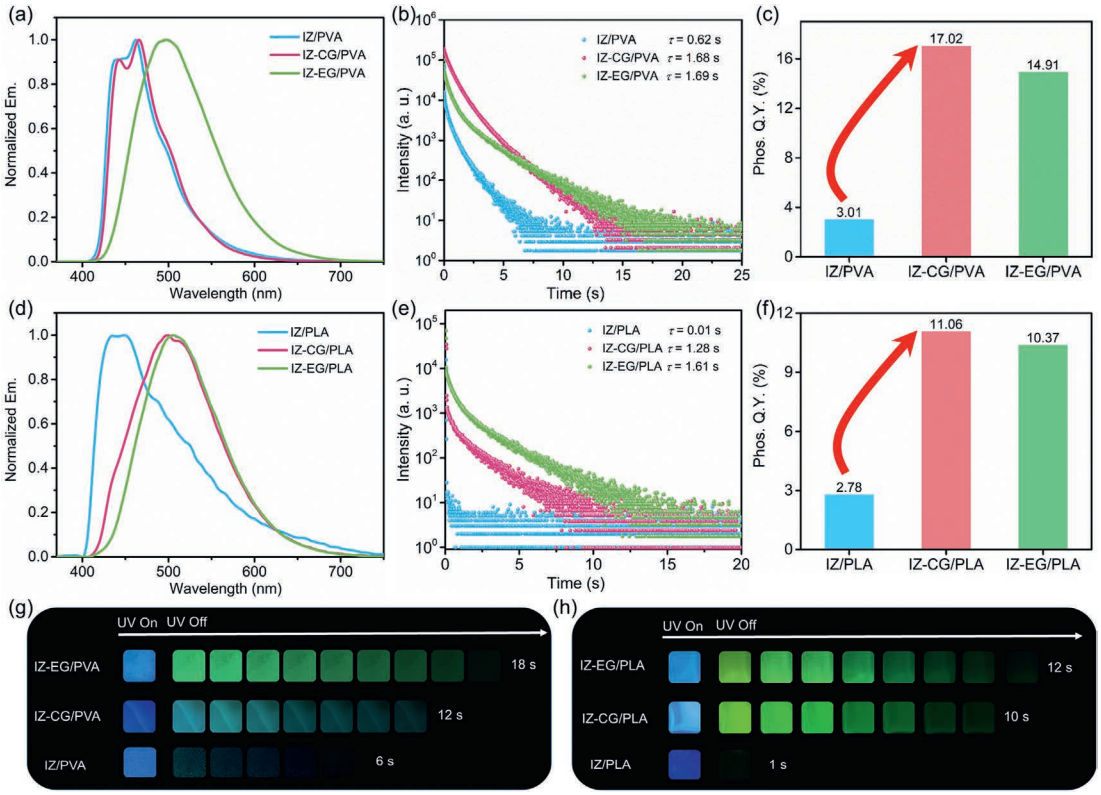


Fig. 3. Phosphorescence emission spectra (a), emission intensity decay curves (b) and phosphorescence Q.Y. (c) of PVA-based doped materials. Phosphorescence emission spectra (d), emission intensity decay curves (e) and phosphorescence Q.Y. (f) of PLA-based doped materials. (g) Luminescence pictures of PVA-based doped materials before and after turning off the 365 nm light. (h) Luminescence pictures of PLA-based doped materials before and after turning off the 365 nm light (Ex. of PVA-based and PLA-based doped materials: 350 nm, delayed time: 1 ms).

The doped material IZ/TPAs also displayed blue fluorescence emission at 397 nm (fluorescence Q.Y. = 11.46 %), and weak green afterglow at 510 nm (Fig. S6 and Table S1 and Fig. 2d), with a phosphorescence lifetime of 37 ms and a phosphorescence Q.Y. of 5.00 % (Figs. 2e and f). Correspondingly, both doped materials, IZ-CG/TPAs and IZ-EG/TPAs, demonstrated significantly enhanced phosphorescence performance. Specifically, the fluorescence quantum yields improved to 22.74 % and 26.34 % (Table S1), while the phosphorescence quantum yields reached 13.66 % and 15.93 %, respectively (Fig. 2f). Furthermore, the phosphorescence lifetimes were substantially prolonged to 218 and 232 ms (Fig. 2e). In both the PB or TPAs host matrix, the IZ-CG- and IZ-EG-doped materials exhibit significantly higher afterglow intensity and longer afterglow duration (2.5-4 s) than the IZ-doped material (1-1.5 s) upon removal of the excitation source. (Figs. 2g and h). These results demonstrated that the enhancement of guest luminescence performance through carbonyl modification significantly improved the phosphorescence performance of the doped materials. Notably, although the specific groups introduced by the carbonyl-modified guests differ and the selected small molecule hosts were also different, all doped materials exhibited similarly excellent phosphorescence activity, indicated that the incorporation of carbonyl groups into guest molecules is a universal strategy for enhancing the phosphorescence property of doped system.

To further investigate the applicability of carbonyl-modified guests, polymers polyvinyl alcohol (PVA) and polylactic acid (PLA) were chosen as the host matrix. In addition, the introduction of carbonyl groups is beneficial for promoting the formation of hydrogen bonding networks in the doped system, which can suppress the non-radiative decay of excitons, thereby further improving the phosphorescence performance of doped materials [53–57]. We also first evaluated the RTP performance of IZ-EG/PVA films at various doping mass ratios (1:100 to 1:2000) and identified the optimal doping concentration as 1:500 based on the RTP intensity (Fig. S7 in Supporting information). Three doped materials also exhibited dual-mode emission, featuring blue fluorescence at 369 nm of IZ/PVA and 403 nm of IZ-CG/PVA and IZ-EG/PVA (Fig. S8 in Supporting information and Fig. 3a). The fluorescence quantum yield increased from 16.54 % for IZ/PVA to 39.82 % for IZ-CG/PVA and 37.21 % for IZ-EG/PVA (Table S1). The phosphorescence lifetime of IZ/PVA was 620 ms and the phosphorescence quantum efficiency was 3.01 %, while the phosphorescence lifetimes of IZ-CG/PVA and IZ-EG/PVA can reach 1680 ms and 1690 ms (Fig. 3b), and the phosphorescence quantum yields were also as high as 17.02 % and 14.91 % (Fig. 3c). Consistent with the PVA-doped films, the phosphorescence performance of IZ-CG/PLA and IZ-EG/PLA films was also markedly improved compared to that of IZ/PLA film. Three doped materials also exhibited dual-mode emission like PVA-based doped materials (Fig. S8 and Fig. 3d) and the phosphorescence lifetimes had been extended from 10 ms to 1281 ms and 1612 ms (Fig. 3e). Concurrently, the fluorescence quantum yield increased from 14.28 % to 36.97 % and 34.00 % (Table S1), while the phosphorescence quantum yields had been increased from 2.78 % to 11.06 % and 10.37 % (Fig. 3f). Similar to the doped systems with small molecules as the host, polymer doped materials with IZ-CG and IZ-EG as the guest have significantly better phosphorescence performance compared to polymer materials with IZ as the guest (Figs. 3g and h). These results demonstrated that carbonyl-modified guests were not only compatible with doped systems based on small-molecule hosts, but also exhibited outstanding performance in polymer-hosted doped systems. This suggested that the strategy of improving phosphorescence performance through carbonyl modification of organic guests possesses broad applicability.

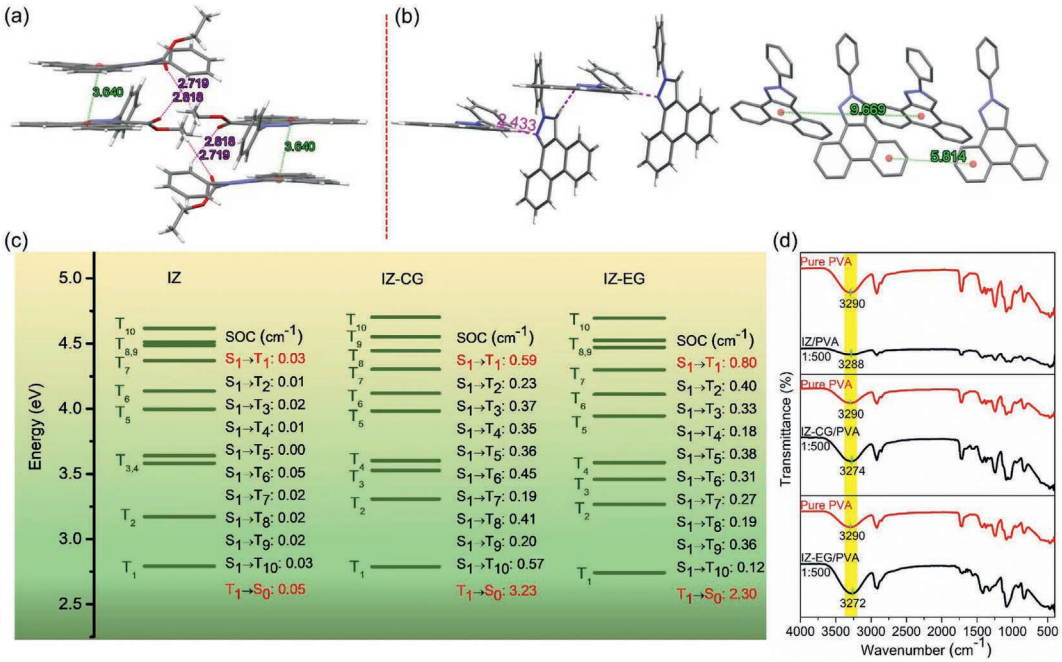


Fig. 4. Single-crystal structures of guests IZ-EG (a) (CCDC: 2448084), IZ (b) (CCDC: 2448083). (c) SOC and energy levels of three guests IZ, IZ-CG and IZ-EG. (d) FT-IR spectra of IZ, IZ-CG and IZ-EG-doped PVA films.

In most doped systems, the strong intermolecular interaction of guests was beneficial for stabilizing the triplet exciton, thereby improving the phosphorescence property of doped materials. Herein, the single crystal structure of the guests indicated that guest with carbonyl group had significantly stronger intermolecular interactions than guest without carbonyl group. As shown in Fig. 4a, in guest molecule IZ-EG, the carbonyl groups in four molecules can form hydrogen bonds resembling a square shape from four directions (top, bottom, left, right), with the distance of only 2.719 and 2.818 Å. In addition, the two IZ-EG guest molecules were arranged almost completely face-to-face in parallel, and the distance between the fused-ring parts of the two guests was 3.640 Å (Fig. 4a), indicating a strong π-π interaction. Such strong hydrogen bonds and π-π interactions can greatly stabilize sensitive triplet excitons, ultimately improving the phosphorescence performance of doped materials. Correspondingly, for guest IZ, there was almost no significant interaction between molecules (Fig. 4b). Two IZ molecules were arranged in a cross shaped almost vertical manner, with almost no face-to-face parts, and the nearest effective distance was up to 5.814 Å. Density functional theory calculations were conducted to further investigate the influence of carbonyl groups on the electronic structure of molecules. The distribution of LUMO (lowest unoccupied molecular orbital) and HOMO (highest occupied molecular orbital) in IZ molecule was almost identical, both distributed throughout the entire molecule. However, for the guest molecules IZ-CG and IZ-EG, due to the introduction of electron withdrawing carbonyl group, although HOMO was still distributed throughout the molecules, the center of gravity of LUMO distribution shifts to the indazole groups and carbonyl groups. In addition, the molecular energy gap had also decreased from 6.33 eV for IZ to 5.43 eV and 5.47 eV for IZ-CG and IZ-EG (Fig. S9 in Supporting information). Carbonyl groups can promote n-π^* transitions, thereby increasing the SOC constant of molecules (Table S2 in Supporting information). The energy level calculation results also conformed to this theory. The SOC between S_1 state and T_1 state was increased from 0.03 cm^{-1} of IZ to 0.59 and 0.80 cm^{-1} of IZ-CG and IZ-CG (Fig. 4c), an increase of up to 19.67-26.67 times, and other SOC between S_1 state and T_n states of IZ-CG and IZ-CG also significantly increased, what is more notable is the SOC constant for the $T_1 \rightarrow S_0$ transition increased significantly from 0.05 cm^{-1} in IZ to 3.23 cm^{-1} in IZ-CG and 2.30 cm^{-1} in IZ-EG (Fig. 4c). Such large SOC obviously help to improve the ISC efficiency of excitons, resulting in the doped materials with IZ-CG and IZ-CG as the guests had better phosphorescence activity. It should be pointed out that the afterglow duration of these carbonyl-modified indazole derivatives in small-molecule doped systems was limited to a maximum of 4 s, whereas doping into polymers PVA and PLA extended the afterglow duration to 18 s, and the highest phosphorescence quantum yield also reached to 17.02 %. This is because the hydrogen bond formed between the carbonyl group in the guests and the hydroxyl/carboxyl groups in the polymers help to suppress the motion of guest molecules, ultimately further enhanced the phosphorescence properties of the doped system. To validate the anchoring effect of hydrogen-bonding interactions, the Fourier-transform infrared (FT-IR) spectra of pure PVA, IZ/PVA, IZ-EG/PVA, and IZ-CG/PVA films were measured (Fig. 4d). Compared to the pure PVA film, the hydroxyl stretching vibration peak of the IZ-EG/PVA and IZ-CG/PVA films shifted to a lower wavenumber by 18 and 16 cm^{-1} (Fig. 4d), but that of the IZ/PVA film shifted by only 2 cm^{-1} (Fig. 4d). The above results confirmed the formation of hydrogen bonds [58–60] between PVA and the guests IZ-EG and IZ-CG. Furthermore, we selected polystyrene (PS), which lacks hydrogen-bonding sites, as the reference host to prepare doped materials and characterized their photophysical properties. Both IZ-CG/PS and IZ-EG/PS exhibited superior performance in terms of quantum yield and phosphorescence lifetime compared to IZ/PS. The phosphorescence lifetime of IZ/PS, IZ-CG/PS, and IZ-EG/PS was 321, 778, and 819 ms, respectively, and the phosphorescence Q.Y. were 2.52 %, 9.38 %, and 10.95 %, respectively (Fig. S10 in Supporting information). Although these values remain lower than those of PVA and PLA based doped materials, they still represent a significant improvement compared to IZ-CG/PB. Therefore, the significant enhancement of phosphorescence property in PVA and PLA host matrices was due to the dual support of hydrogen bonds and polymer rigidity.

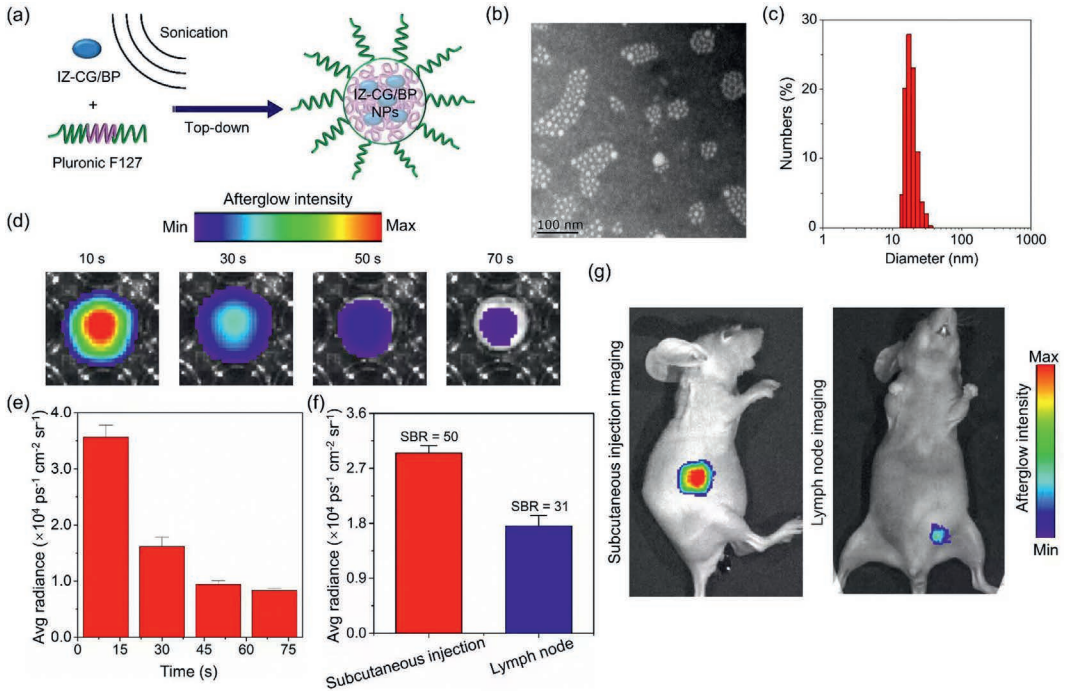


Fig. 5. (a) Schematic diagram of the preparation of IZ-CG/BP NPs *via* a top-down route. (b) TEM image of IZ-CG/BP NPs. Scale bar: 100 nm. (c) Hydrodynamic diameter of IZ-CG/BP NPs determined by DLS. (d) Time-dependent phosphorescence images of various NPs (5 mg/mL) at 37 °C post UV-light pre-irradiation for 70 s, acquired by an IVIS instrument in bioluminescent mode (Ex.: 365 nm). (e) Quantitative analysis based on the typical phosphorescence images in (d). (f) Signal-to-background ratio for phosphorescence intensities in (e). Data mean ± SD ($n = 3$). (g) Afterglow imaging of mice with the subcutaneous injections (left) and lymph nodes (right) of IZ-CG/BP NPs (50 μL, 5 mg/mL, Ex.: 365 nm).

Given the excellent phosphorescence performance of the IZ-CG/BP doped material, the IZ-CG/BP nanoparticles (NPs) were co-encapsulated with the amphiphilic co-polymer F127 as the matrix *via* a nanoprecipitation method (Fig. 5a). IZ-CG/BP NPs with encapsulated concentrations of 5 mg/mL were prepared. Dynamic light scattering and transmission electron microscopy techniques were performed to determine the size and shape of the IZ-CG/BP NPs. The results showed that the NPs exhibited a uniform spherical shape and a mean hydrodynamic diameter of approximately 20 nm (Figs. 5b and c). Following a 70 s UV-light pre-irradiation period, the phosphorescence signals detected through IVIS exhibited strong phosphorescence intensity and 100 s afterglow time for IZ-CG/BP NPs (Figs. 5d and e). Furthermore, stability and toxicity evaluations of the prepared IZ-CG/BP NPs revealed good stability and negligible cytotoxicity (Fig. S11 in Supporting information). Subsequently, *in vivo* phosphorescence imaging experiments were conducted in live mice. All animal studies were performed in compliance with the guidelines set by Tianjin Committee of Use and Care of Laboratory Animals, the overall project protocols were approved by the Animal Ethics Committee of Tianjin University (No. TJUE-2025-105). BALB/c nude mice were injected subcutaneously with IZ-CG/BP NPs. First, the mice were promptly irradiated with a 365 nm UV-lamp for 70 s, then an IVIS was used to observe the resultant afterglow intensity. Fig. 5g showed the subcutaneous phosphorescence imaging results of BALB/c nude mice, and the results indicated that IZ-CG/BP NPs demonstrated a robust phosphorescence intensity, with an SBR reaching 50 (Fig. 5f). We further studied the effect of IZ-CG/BP NPs on lymph node imaging in BALB/c nude mice. BALB/c nude mice were administered IZ-CG/BP NPs *via* paw injection, after 15 min, the mice were subjected to UV-light pre-irradiation for 70 s. The resulting afterglow intensity was quantified using IVIS (Fig. 5g). Similarly, IZ-CG/BP NPs demonstrated great durability of phosphorescence signals and a high SBR of 31 (Fig. 5f). These findings suggest that IZ-CG/BP NPs exhibit superior performance in bioimaging applications, making the doped system potential for future biological research.

In this study, we synthesized two carbonyl-based guest molecules (IZ-CG and IZ-EG) by incorporating carbonyl groups into the indazole derivative IZ. The incorporation of carbonyl groups promotes n-π^* transitions of electrons, significantly enhancing the SOC of the guest molecules, thereby improving the ISC efficiency of excitons. Furthermore, the incorporation of carbonyl groups facilitates the formation of hydrogen bonds between the guest and host molecules, thereby strengthening their interactions. Consequently, the incorporation of carbonyl groups not only enhances the phosphorescence intensity of the doped materials but also prolongs their afterglow duration. The phosphorescence Q.Y. and lifetime of the doped material with IZ as the guest were 2.78 %-7.20 % and 10-620 ms, respectively, while those of the doped materials with carbonyl-modified guests increased to 10.37 %-21.41 % and 218-1690 ms. Finally, the doped material was successfully used for imaging subcutaneous and lymph nodes in mice. This work demonstrated that the incorporation of carbonyl groups into organic guest molecules represented an effective strategy for enhancing the phosphorescence performance of doped system.

Declaration of competing interest

The authors declare that they have no known competing financial interests or personal relationships that could have appeared to influence the work reported in this paper.

CRediT authorship contribution statement

Lei Wang: Writing – original draft, Methodology, Investigation, Formal analysis, Conceptualization. **Jianing Zhang:** Methodology, Investigation. **Jin Xiong:** Investigation. **Wenbo Dai:** Funding acquisition, Formal analysis. **Miaochang Liu:** Resources, Project ad-

ministration. **Xiaobo Huang:** Writing – original draft, Methodology, Funding acquisition, Formal analysis, Conceptualization. **Yuye Chai:** Resources. **Yunxiang Lei:** Writing – review & editing, Supervision, Resources, Project administration, Funding acquisition. **Zhengxu Cai:** Supervision, Resources, Conceptualization. **Minyu Zhu:** Funding acquisition, Formal analysis, Conceptualization.

Acknowledgments

This work is supported by the National Natural Science Foundation of China (Nos. 22405194, 22105148), the Zhejiang Provincial Natural Science Foundation of China (No. LY21H070003), and the Basic Research Project of Wenzhou City, China (No. Y20220923).

Supplementary materials

Supplementary material associated with this article can be found, in the online version, at doi:10.1016/j.cclet.2025.111706.

References

[1] Y. Wang, H. Gao, J. Yang, et al., Adv. Mater. 33 (2021) 2007811.
[2] J. Zhou, D. Liu, L. Li, et al., Chin. Chem. Lett. 35 (2024) 109929.
[3] F. Xiao, H. Gao, Y. Lei, et al., Nat. Commun. 13 (2022) 186.
[4] G. Yang, S. Hao, Y. Dan, et al., Adv. Mater. 37 (2025) 2418042.
[5] Y. Zhang, H. Li, M. Yang, et al., Chem. Commun. 59 (2023) 5329–5342.
[6] M. Ghasemi, M. Mahmoudi, D. Gudeika, et al., Chem. Eng. J. 473 (2023) 145004.
[7] F. Guo, Y. Chen, C. Li, et al., Adv. Funct. Mater. 35 (2024) 2416465.
[8] H. Yao, F. Yang, J. hu, et al., Chin. Chem. Lett. 36 (2025) 110375.
[9] F. Nie, D. Yan, Nat. Commun. 15 (2024) 9491.
[10] H. Sun, Y. Xiao, Y. He, et al., Chem. Sci. 16 (2025) 5299–5309.
[11] S. Sun, Y. Zhu, T. Li, et al., Chem. Eng. J. 485 (2024) 149751.
[12] W. Dai, G. Li, Y. Zhang, et al., Adv. Funct. Mater. 33 (2022) 2210102.
[13] L. Li, J. Zhou, J. Han, et al., Nat. Commun. 15 (2024) 3746.
[14] D. Wang, J. Gong, Y. Xiong, et al., Adv. Funct. Mater. 33 (2022) 2208895.
[15] G. Baryshnikov, B. Minaev, H. Ågren, et al., Chem. Rev. 117 (2017) 6500–6537.
[16] J. Li, X. Li, G. Wang, et al., Nat. Commun. 14 (2023) 1987.
[17] Z. Chen, J. Shi, Y. Zhou, P. Zhang, G. Liang, Chin. Chem. Lett. 36 (2025) 110629.
[18] J. Li, X. Wang, Y. Pan, et al., Chem. Commun. 57 (2021) 8794–8797.
[19] M. Wang, F. Li, Y. Lei, et al., Chem. Eng. J. 429 (2022) 132288.
[20] Z. Chai, C. Wang, J. Wang, et al., Chem. Sci. 8 (2017) 8336–8344.
[21] M. Fang, J. Yang, X. Xiang, et al., Mater. Chem. Front. 2 (2018) 2124–2129.
[22] D. Li, F. Lu, J. Wang, et al., J. Am. Chem. Soc. 140 (2018) 1916–1923.
[23] N. Liu, Y. Pan, Y. Lei, et al., Chem. Eng. J. 433 (2022) 133530.
[24] H. Yang, Y. Wang, X. Yao, et al., J. Am. Chem. Soc. 147 (2024) 1474–1481.
[25] Y. Gong, G. Chen, Q. Peng, et al., Adv. Mater. 27 (2015) 6195–6201.
[26] L. Gu, H. Shi, C. Miao, et al., J. Mater. Chem. C 6 (2018) 226–233.
[27] Y. Chen, Y. Xie, H. Shen, et al., Chem. Eur. J. 26 (2020) 17376–17380.
[28] Y. Lei, W. Dai, J. Guan, et al., Angew. Chem. Int. Ed. 59 (2020) 16054–16060.
[29] Y. Lei, J. Yang, W. Dai, et al., Chem. Sci. 12 (2021) 6518–6525.
[30] X. Liu, Y. Pan, Y. Lei, et al., J. Phys. Chem. Lett. 12 (2021) 7357–7364.
[31] D. Wang, Y. Xie, X. Wu, et al., J. Phys. Chem. Lett. 12 (2021) 1814–1821.
[32] F. Xiao, M. Wang, Y. Lei, et al., J. Mater. Chem. C 8 (2020) 17410–17416.
[33] S. Cai, H. Ma, H. Shi, et al., Nat. Commun. 10 (2019) 4247.
[34] Z. Cheng, H. Shi, H. Ma, et al., Angew. Chem. Int. Ed. 57 (2017) 678–682.
[35] W. Dai, Y. Jiang, Y. Lei, et al., Chem. Sci. 15 (2024) 4222–4237.
[36] J. Wang, X. Gu, H. Ma, et al., Nat. Commun. 9 (2018) 2963.
[37] Z. Zhao, X. Liu, W. Dai, et al., J. Phys. Chem. Lett. 15 (2024) 8093–8100.
[38] R. Kabe, C. Adachi, Nature 550 (2017) 384–387.
[39] A. Mazarevics, K. Leduskrasts, ACS Mater. Lett. 6 (2024) 2703–2713.
[40] W. Yuan, Y. Shen, H. Zhao, et al., J. Phys. Chem. C 114 (2010) 6090–6099.
[41] H. Wu, C. Hang, X. Li, et al., Chem. Commun. 53 (2017) 2661–2664.
[42] Y. Xie, Y. Ge, Q. Peng, et al., Adv. Mater. 29 (2017) 1606829.
[43] Y. Xiong, Z. Zhao, W. Zhao, et al., Angew. Chem. Int. Ed. 57 (2018) 7997–8001.
[44] X. Zhang, T. Xie, M. Cui, et al., ACS Appl. Mater. Interfaces 6 (2014) 2279–2284.
[45] W. Zhao, Z. He, Jacky W.Y. Lam, et al., Chem 1 (2016) 592–602.
[46] Y. Huang, Y. Liu, X. Zheng, et al., Adv. Opt. Mater. 13 (2025) 2500743.
[47] X. Zheng, Y. Huang, W. Lv, et al., Angew. Chem. Int. Ed. 61 (2022) e202207104.
[48] K. Chen, Y. Jiang, Y. Zhu, et al., J. Mater. Chem. C 10 (2022) 11607–11613.
[49] Y. Guo, K. Chen, Z. Hu, et al., J. Phys. Chem. Lett. 13 (2022) 7607–7617.
[50] Y. Jiang, C. Zhang, R. Wang, et al., Adv. Opt. Mater. 12 (2023) 2302482.
[51] X. Liu, W. Dai, J. Qian, et al., J. Mater. Chem. C 9 (2021) 3391–3395.
[52] J. Qian, W. Dai, X. Qiu, et al., Mater. Chem. Front. 9 (2025) 818–827.
[53] S. Cai, Z. Sun, H. Wang, et al., J. Am. Chem. Soc. 143 (2021) 16256–16263.
[54] Y. Dai, R.A. Somoza, L. Wang, et al., Angew. Chem. Int. Ed. 58 (2019) 17399–17405.
[55] C. Ren, Z. Wang, T. Wang, et al., Chin. J. Chem. 40 (2022) 1987–2000.
[56] Y. Zhang, Z. Wang, Y. Su, et al., Research 2021 (2021) 8096263.
[57] Z.Y. Zhang, W.W. Xu, W.S. Xu, et al., Angew. Chem. Int. Ed. 59 (2020) 18748–18754.
[58] Q. Liu, X. Liu, X. Yu, et al., Angew. Chem. Int. Ed. 63 (2024) e202403391.
[59] Y.J. Wang, X.N. Zhang, Y. Song, et al., Chem. Mater. 31 (2019) 1430–1440.
[60] J. You, X. Zhang, Q. Nan, et al., Nat. Commun. 14 (2023) 4163.